JACS
JOURNAL OF THE AMERICAN CHEMICAL SOCIETY
Communication
pubs.acs.org/JACS

A Stable Coordination Complex of Rh(IV) in an N,O-Donor Environment

Shashi B. Sinha,[†] Dimitar Y. Shopov,[†] Liam S. Sharninghausen,[†] David J. Vinyard, Brandon Q. Mercado, Gary W. Brudvig,* and Robert H. Crabtree*

Department of Chemistry, Yale University, 225 Prospect Street, New Haven, Connecticut 06520, United States

Supporting Information

ABSTRACT: We describe facial and meridional isomers of $[Rh^{III}(pyalk)_3]$, as well as meridional $[Rh^{IV}(pyalk)_3]^+$ {pyalk =2-(2-pyridyl)-2-propanoate}, the first coordination complex in an N,O-donor environment to show a clean, reversible $Rh^{III/IV}$ redox couple and to have a stable Rh(IV) form, which we characterize by EPR and UV−visible spectroscopy as well as X-ray crystallography. The unprecedented stability of the Rh(IV) species is ascribed to the exceptional donor strength of the ligands, their oxidation resistance, and the meridional coordination geometry.

Interest in high oxidation state transition-metal complexes has grown considerably in recent years in connection with oxidation catalysis.[1] While there are a number of well-established Ir(IV) complexes, the highest oxidation state commonly encountered for rhodium is Rh(III).[2,3] Among the very few Rh(IV) species known, $[RhX_6]^{2-}$ (X = Cl, F) is unstable in water, which has limited its characterization.[4] There are also a number of poorly characterized solid-state Rh(IV) oxide species[5] as well as several formally Rh(IV) dinuclear organometallic compounds.[6] Several other complexes, such as Claus' Blue, originally thought to feature Rh(IV), are in fact superoxides of Rh(III).[7] Rh(IV) species have been postulated as intermediates in chemical transformations,[8] and characterization of a stable Rh(IV) complex is, therefore, of interest. However, there do not seem to be any examples of well-characterized stable coordination compounds of Rh(IV) with organic ligands; a few reports of metastable Rh(IV) species present only very limited characterization.[9] A common problem with these and other highly oxidized complexes is oxidative instability of the organic ligands, which limits the formation of stable species.[10]

We recently reported that the oxidatively robust, bidentate pyridine-alkoxide ligand pyalk (2-(2-pyridyl)-2-propanoate) strongly stabilizes high oxidation states.[3] Both the facial and meridional isomers of $Ir(pyalk)_3^{0/+}$ had easily accessible III/IV couples, with the meridional isomer having what may be the lowest $Ir^{III/IV}$ reduction potential ever reported. In water-oxidation catalysis,[11] pyalk displays extremely high stability even under harsh catalytic conditions. We now report an extension of these observations to the stabilization of the more challenging Rh(IV) oxidation state. The meridional ($\mathbf{1}^{III}$) and facial ($\mathbf{2}^{III}$) isomers of $[Rh^{III}(pyalk)_3]$ (Scheme 1) can be synthesized, separated, and characterized. The *mer* isomer shows a reversible electrochemical redox couple and can be cleanly

Scheme 1. Preparation of Complexes $\mathbf{1}^{III}$, $\mathbf{2}^{III}$, and $[\mathbf{1}^{IV}]SbF_6$

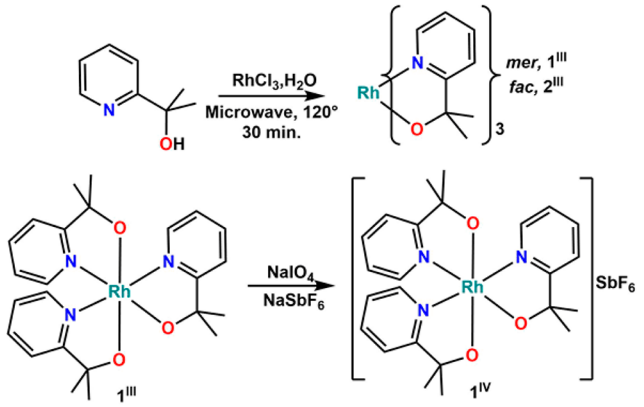

chemically oxidized to the corresponding $[Rh^{IV}(pyalk)_3]^+$ species, which proves to be kinetically stable in a range of solvents including water. Full characterization, including the first clear and well-simulated Rh(IV) EPR spectrum as well as the first crystal structure of a Rh(IV) coordination complex with organic ligands, establishes the identity of this complex.

Compounds $\mathbf{1}^{III}$ and $\mathbf{2}^{III}$ were prepared by microwave heating an aqueous solution of $RhCl_3$ with an excess of Hpyalk (Scheme 1). With excess ligand as the base, clean conversion occurs without formation of metal oxides. Separation of $\mathbf{1}^{III}$ and $\mathbf{2}^{III}$ is possible due to their disparate polarities (see SI). Both $\mathbf{1}^{III}$ and $\mathbf{2}^{III}$ were isolated as air-stable yellow powders exhibiting a remarkably broad solubility range and were fully characterized. $\mathbf{1}^{III}$ is the major product of the reaction (9:1 ratio vs $\mathbf{2}^{III}$ based on ^1H NMR of the crude mixture; 60% isolated yield), while $\mathbf{2}^{III}$ is the minor product (2% isolated yield). The complexes display the ^1H and ^{13}C NMR signals (see SI) expected from their symmetry, with three sets of ligand signals for $\mathbf{1}^{III}$ and only one for $\mathbf{2}^{III}$. The methyl groups of the ligands are inequivalent in both ^1H and ^{13}C NMR, as expected.

Addition of sodium periodate to a solution of $\mathbf{1}^{III}$ causes a color change from pale yellow to dark purple over ∼20 min. This new species can be extracted into dichloromethane and crystallized, after addition of SbF_6^-, to give $[\mathbf{1}^{IV}]SbF_6$ as a dark violet solid. This rare Rh(IV) complex shows much greater stability in both aqueous and oxidation-resistant organic solvents than previous Rh(IV) coordination compounds.[9] At room temperature,

Received: November 19, 2015
Published: December 7, 2015

ACS Publications © 2015 American Chemical Society

DOI: 10.1021/jacs.5b12148
J. Am. Chem. Soc. 2015, 137, 15692−15695

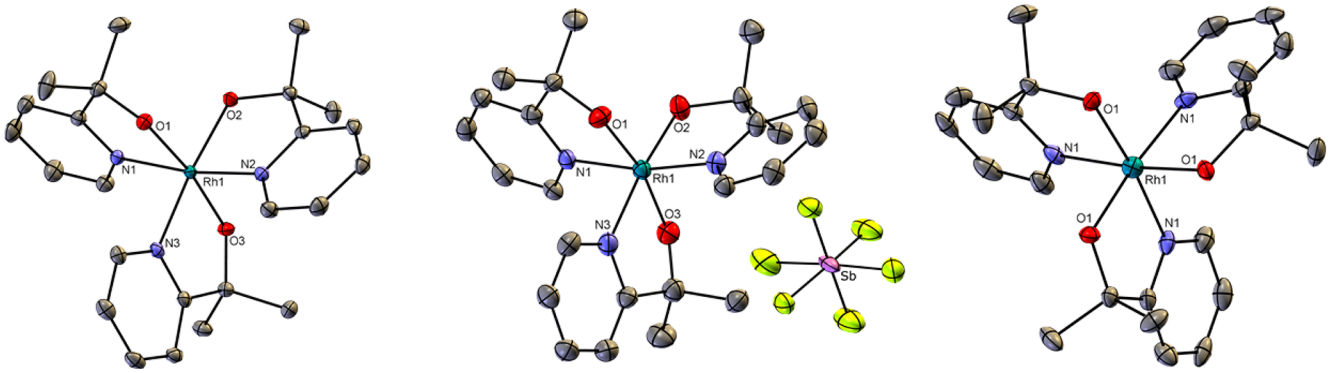

Figure 1. Thermal ellipsoid diagrams of the crystal structures of $\mathbf{1}^{III}$ (left, at 50% probability level), $[\mathbf{1}^{IV}]SbF_6$ (center), and $\mathbf{2}^{III}$ (left) at 30% probability level. Hydrogen atoms have been omitted for clarity.

degradation proceeds over the course of several days and primarily involves the reversible reduction to $\mathbf{1}^{III}$, a process also achieved with chemical reductants like sodium ascorbate. In contrast, attempts to oxidize $\mathbf{2}^{III}$ did not result in an isolable species. This difference in redox properties is consistent with our findings for the Ir analogues.

Crystal structures were obtained for $\mathbf{1}^{III}$, $[\mathbf{1}^{IV}]SbF_6$, and $\mathbf{2}^{III}$ (Figure 1). The Rh−O bonds contract noticeably (by ∼0.08 Å on average) upon oxidation (Table 1), consistent with a metal-centered process, while the Rh−N bonds undergo a slight extension, trends that are in line with the analogous Ir complexes.[3] To our knowledge, the structure of $[\mathbf{1}^{IV}]SbF_6$ represents the first example of a crystal structure of a molecular Rh(IV) coordination complex with organic ligands. Complex $\mathbf{1}^{III}$ crystallizes as a well-ordered monohydrate. Complex $\mathbf{2}^{III}$ demonstrates high cation affinity by coordinating to Na^+ ions with its facial alkoxide groups; chloride counterions and disordered dichloromethane molecules are also present (see SI).

Table 1. Comparison of Selected Crystallographic Bond Distances in $\mathbf{1}^{III}$ and $[\mathbf{1}^{IV}]SbF_6$

bond	$\mathbf{1}^{III}$	$[\mathbf{1}^{IV}]SbF_6$[a]
Rh1−N1	2.019(1)	2.025(5)
Rh1−N2	2.015(1)	2.027(6)
Rh1−N3	2.029(1)	2.063(5)
Rh1−O1	2.022(1)	1.920(5)
Rh1−O2	1.990(1)	1.923(6)
Rh1−O3	2.044(1)	1.965(5)

[a]Bond lengths calculated as average of lengths in the two molecules in the asymmetric unit.

While the UV−visible spectrum (Figure 2) of $\mathbf{1}^{III}$ only shows a weak absorption tail in the visible region, the oxidized state shows three peaks, the strongest at 520 nm having $\varepsilon = 2500\ M^{-1}cm^{-1}$. These peaks are assigned to ligand-to-metal charge transfers by analogy with Ir(IV) species; the Rh(IV) spectrum closely resembles the Ir analog's, but is red-shifted by ∼100−150 nm.[3]

Electron paramagnetic resonance (EPR) spectroscopy on $\mathbf{1}^{IV}$ (Figure 3) provides further evidence for the Rh(IV) state. Consistent with the proposed $S = 1/2$ system, a rhombic signal is evident which displays hyperfine coupling to ^{103}Rh ($I = 1/2$), resolved as doublets in the midfield and high-field peaks. The magnitude of the ^{103}Rh hyperfine coupling and the breadth of the signal are strongly indicative of a metal-centered electron spin. Coupling to ^{14}N is not observed, consistent with calculations on the analogous Ir complex that showed essentially no frontier orbital occupancy on N.[3] The spectrum was successfully simulated by considering only the ^{103}Rh coupling and diffuse hyperfine strain (Figure 3). This seems to be the first example of a clean, solution-phase Rh(IV) EPR spectrum for which Rh coupling is resolved.

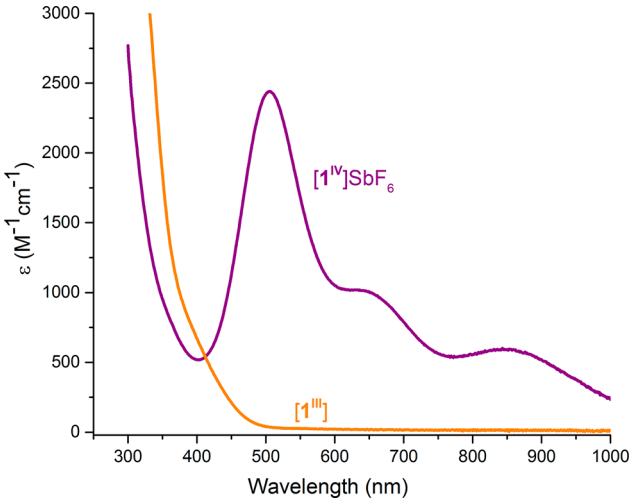

Figure 2. UV−vis absorption spectra of $[\mathbf{1}^{III}]$ (orange) and $[\mathbf{1}^{IV}]SbF_6$ (purple) in dichloromethane.

In cyclic voltammetry, each isomer shows only one redox feature in the range studied, but at significantly different potentials. For **1**, a fully reversible feature at 0.98 V vs NHE (pH 7, phosphate buffer) is observed with cathodic and anodic currents essentially equal at all scan rates (Figure 4) and with the expected square-root relationship between peak current and scan rate. The symmetry between anodic and cathodic waves supports the reversible nature of this feature, which we assign as the $Rh^{III/IV}$ couple. While there is a noticeable rise in the peak-to-peak separation at higher scan rates, this is likely due to slow electron transfer at the working electrode, boron-doped diamond (BDD). Although BDD is known to have substantially slower electron transfer kinetics than more common electrodes,[12] it is better adapted for aqueous work at these high potentials, having much lower background current. In contrast to **1**, the redox feature for **2** is only quasi-reversible (see SI). Due to its very high potential (1.38 V vs NHE), as well as an underlying catalytic wave (presumably degradation), the oxidized state is most likely short-lived under these conditions. While no characterization has been attempted so far, we tentatively attribute this feature to a $Rh^{III/IV}$ couple as well.

DOI: 10.1021/jacs.5b12148
J. Am. Chem. Soc. 2015, 137, 15692−15695

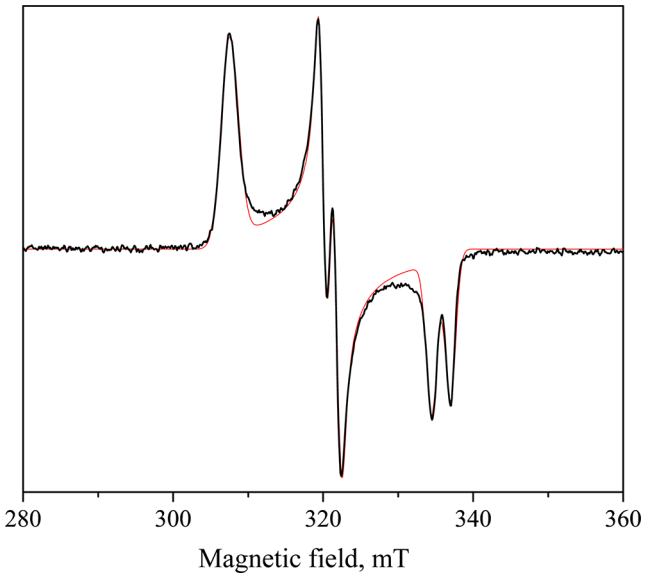

Figure 3. X-band EPR spectrum of compound $\mathbf{1}^{IV}$ measured at 8 K (black) and simulation (red). Compound $\mathbf{1}^{IV}$ has a rhombic EPR spectrum with g = [2.180, 2.089, 1.997] consistent with low-spin (S = 1/2) Rh(IV). Hyperfine interactions from the I = 1/2 ^{103}Rh nucleus (100%) were simulated using principal values of 31, 53, and 70 MHz. Anisotropic line broadening was simulated using the H-strain tensor [70, 33, 44] MHz to account for unresolved hyperfine interactions.

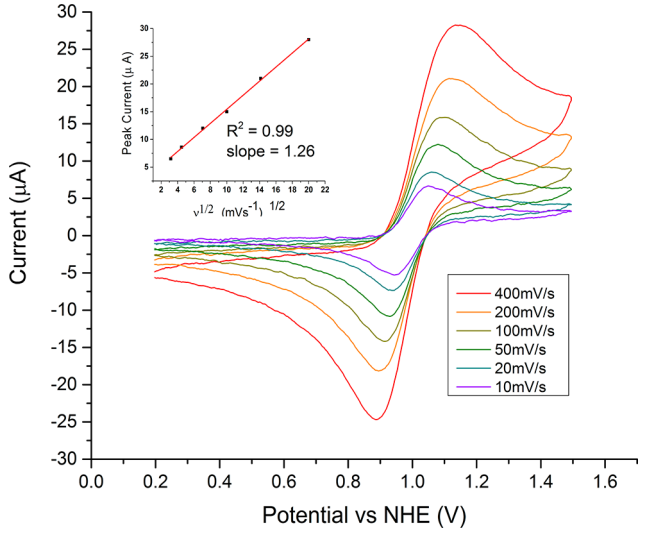

Figure 4. Cyclic voltammograms of **1** in 0.1 M phosphate buffer at pH 7.0 at different scan rates from 10 to 400 mV s^{-1}. Insert: plot of peak current versus (scan rate)$^{1/2}$.

The $Rh^{III/IV}$ couples are pH dependent, suggesting that the alkoxide groups in the Rh(III) state are sufficiently basic to be partially protonated even at neutral pH. The Pourbaix curve for the $Rh^{III/IV}$ couple of **1** (Figure 5) indicates a proton-dependent (1 H^+/e^-) electron-transfer regime below pH 7 and a proton-independent regime above pH 8. Based on the basicity of the alkoxide, we assign the Rh(III) species in acid as monoprotonated $[\mathbf{1}^{III}\mathbf{H}]^+$, in base as $\mathbf{1}^{III}$, and in the oxidized state as the pH-invariant $[\mathbf{1}^{IV}]^+$. Because basic conditions provide a stable regime involving two well-defined species, we can compare the aqueous $Rh^{III/IV}$ potential for $\mathbf{1}^{III}$ at 0.935 V vs NHE with that for $\mathbf{2}^{III}$ with $E_{1/2}$ = 1.28 V at pH 11, their separation being 0.345 V. We will use these as the formal aqueous $Rh^{III/IV}$ potentials. Both the *mer*/*fac* isomer separation and the features of the Pourbaix curve very closely mirror those for the Ir(pyalk)$_3$ complexes,[3] the primary difference being the Rh/Ir offset, of ∼0.5 V. The lack of perfect linearity in the pH = 3−7 range is attributed to the highly basic character of the alkoxide ligands that promotes pH-dependent hydrogen bonding and ion binding, as also observed for the Ir analog.[3]

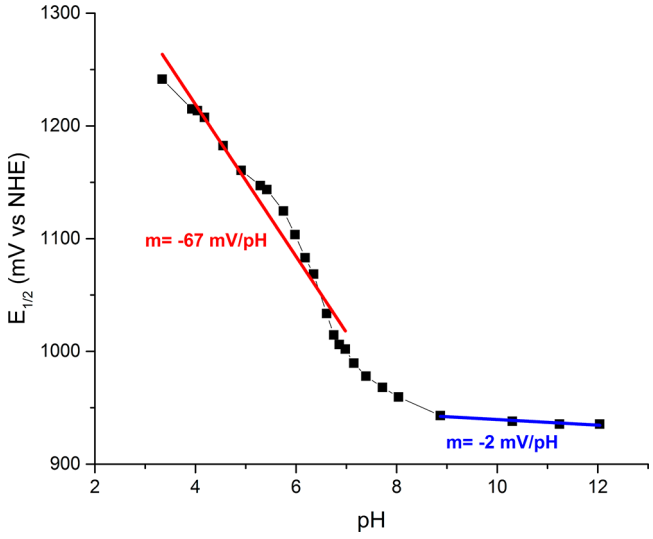

Figure 5. The pH dependence of the $Rh^{III/IV}$ electrochemical redox couple for **1**. Linear regression fits and their slopes are given for data points pH < 7 (red) and pH > 8 (blue).

The reasons our *mer* complex avoids the typical instability of the Rh(IV) state are the strong donor and oxidation-resistant tertiary alkoxide ligands as well as the meridional geometry itself. For iridium, alkoxides can be extremely potent donors, surpassing even phenyl ligands;[3,13] this has been ascribed to their dual σ- and π-donating character. Furthermore, we and others[3,11] have shown the importance of ligand orientation on redox properties. The ease of oxidation depends not only on the sum of the donor effects of the ligand groups, following Lever,[14] but also on the electronic splitting of the otherwise degenerate t_{2g} d-orbitals. A $d^6 \rightarrow d^5$ oxidation of a pseudo-octahedral complex is facilitated when one orbital energy is raised via this splitting. Because the t_{2g} orbitals are planar in shape, the greatest effect occurs when the most electron-donating ligands all lie in one plane. In our case, all three alkoxides occupy one plane in the *mer* complex **1**, whereas for the symmetric *fac* complex **2**, all planes, and thus all t_{2g} orbitals, are equivalent. The net result is that **1** experiences this anisotropic oxidation enhancement effect that splits the t_{2g} d-orbitals, while **2** does not. Although the magnitude of the effect is essentially the same for Rh and Ir, the practical implications for Rh(pyalk)$_3$ are far more impressive: one isomer ($\mathbf{1}^{III}$) forms an unprecedentedly stable and long-lived Rh(IV) species, while the other ($\mathbf{2}^{III}$) forms one only transiently.

In conclusion, we have prepared and characterized *mer*-$[Rh^{III}(pyalk)_3]$, a rhodium coordination complex capable of accessing the rare Rh(IV) oxidation state through both chemical and electrochemical oxidation. In contrast to the previously known Rh(IV) coordination complexes, *mer*-$[Rh^{IV}(pyalk)_3]$ is stable for long periods in a range of solvents. This facilitates characterization by several methods including unprecedented X-ray crystallography and EPR spectroscopy for the Rh(IV) state. The remarkable stability of this complex arises from the strongly donating ligand set, the oxidation-resistant nature of the ligand,

DOI: 10.1021/jacs.5b12148
J. Am. Chem. Soc. 2015, 137, 15692−15695

and the meridional ligand arrangement. The importance of this last aspect is illustrated by the inability of the compositionally equivalent facial isomer, *fac*-[Rh^{III}(pyalk)$_3$], to form a stable Rh(IV) state, showing that coordination geometry can be a critical factor in oxidation state stability.

■ ASSOCIATED CONTENT

Supporting Information

The Supporting Information is available free of charge on the ACS Publications website at DOI: 10.1021/jacs.5b12148.

Figures as well as detailed procedures and methods (PDF)
Crystal structure data (CIF)
Crystal structure data (CIF)
Crystal structure data (CIF)

■ AUTHOR INFORMATION

Corresponding Authors

*robert.crabtree@yale.edu
*gary.brudvig@yale.edu

Author Contributions

†These authors contributed equally.

Notes

The authors declare no competing financial interest.

■ ACKNOWLEDGMENTS

This work was supported the U.S. Department of Energy, Office of Science, Office of Basic Energy Sciences, Division of Chemical Sciences, Geosciences, and Biosciences under award no. DE-SC0001059 as part of the Argonne-Northwestern Solar Energy Research (ANSER) Energy Frontier Research Center (spectroscopy and characterization) and under award no. DEFG02-07ER15909 (synthesis).

■ REFERENCES

(1) (a) Wang, G. J.; Zhou, M. F.; Goettel, J. T.; Schrobilgen, G. J.; Su, J.; Li, J.; Schloder, T.; Riedel, S. *Nature* **2014**, *514*, 475. (b) Sinha, W.; Sommer, M. G.; Deibel, N.; Ehret, F.; Bauer, M.; Sarkar, B.; Kar, S. *Angew. Chem., Int. Ed.* **2015**, *54*, 13769. (c) Sheldon, R. A.; Kochi, J. K. *Metal-Catalyzed Oxidations of Organic Compounds: Mechanistic Principles and Synthetic Methodology Including Biochemical Processes*; Academic Press: New York, 1981. (d) Jørgensen, C. K. *Oxidation numbers and Oxidation States*; Springer: Heidelberg, Germany, 1969. (e) Donoghue, P. J.; Tehranchi, J.; Cramer, C. J.; Sarangi, R.; Solomon, E. I.; Tolman, W. B. *J. Am. Chem. Soc.* **2011**, *133*, 17602. (f) Topczewski, J. J.; Sanford, M. S. *Chem. Sci.* **2015**, *6*, 70.

(2) (a) Gulliver, D. J.; Levason, W. *Coord. Chem. Rev.* **1982**, *46*, 1. (b) Jardine, F. H. *Rhodium: Inorganic & Coordination Chemistry*; John Wiley & Sons Ltd.: Hoboken, NJ, 2006. (c) Campos, J.; Esqueda, A. C.; Lopez-Serrano, J.; Sanchez, L.; Cossio, F. P.; de Cozar, A.; Alvarez, E.; Maya, C.; Carmona, E. *J. Am. Chem. Soc.* **2010**, *132*, 16765. (d) Sewell, L. J.; Lloyd-Jones, G. C.; Weller, A. S. *J. Am. Chem. Soc.* **2012**, *134*, 3598.

(3) Shopov, D. Y.; Rudshteyn, B.; Campos, J.; Batista, V. S.; Crabtree, R. H.; Brudvig, G. W. *J. Am. Chem. Soc.* **2015**, *137*, 7243.

(4) (a) Wilhelm, V.; Hoppe, R. *Z. Anorg. Allg. Chem.* **1974**, *407*, 13. (b) Ellison, I. J.; Gillard, R. D. *Polyhedron* **1996**, *15*, 339.

(5) (a) Bayer, G.; Wiedemann, H. G. *Thermochim. Acta* **1974**, *15*, 213. (b) Muller, O.; Rustum, R. *J. Less-Common Met.* **1968**, *16*, 129. (c) Shannon, R. D. *Solid State Commun.* **1968**, *6*, 139. (d) Vente, J. F.; Lear, J. K.; Battle, P. D. *J. Mater. Chem.* **1995**, *5*, 1785.

(6) (a) Meanwell, N. J.; Smith, A. J.; Maitlis, P. M. *J. Chem. Soc., Dalton Trans.* **1986**, 1419. (b) Wang, Z. Q.; Turner, M. L.; Taylor, B. F.; Maitlis, P. M. *Polyhedron* **1995**, *14*, 2767. (c) Osakada, K.; Koizumi, T.; Yamamoto, T. *Bull. Chem. Soc. Jpn.* **1997**, *70*, 189. (d) Isobe, K.; Okeya, S.; Meanwell, N. J.; Smith, A. J.; Adams, H.; Maitlis, P. M. *J. Chem. Soc., Dalton Trans.* **1984**, 1215.

(7) (a) Ellison, I. J.; Gillard, R. D. *J. Chem. Soc., Chem. Commun.* **1992**, 851. (b) Edwards, N. S. A.; Ellison, I. J.; Gillard, R. D.; Mile, B.; Maher, J. *Polyhedron* **1993**, *12*, 371.

(8) (a) Pestovsky, O.; Bakac, A. *Inorg. Chem.* **2002**, *41*, 3975. (b) Pestovsky, O.; Bakac, A. *Inorg. Chem.* **2002**, *41*, 901. (c) Pestovsky, O.; Bakac, A. *J. Am. Chem. Soc.* **2002**, *124*, 1698. (d) Kim, M. Y.; Seok, W. K.; Dong, Y.; Yun, H. *Inorg. Chim. Acta* **2001**, *319*, 194.

(9) (a) Basu, S.; Peng, S.-M.; Lee, G.-H.; Bhattacharya, S. *Polyhedron* **2005**, *24*, 157. (b) Lee, W.-T. Ph.D. Thesis, University of Iowa, Iowa City, IA, 2011. (c) Bond, A. M.; Colton, R.; Mann, D. R. *Inorg. Chem.* **1990**, *29*, 4665.

(10) (a) Crabtree, R. H. *J. Organomet. Chem.* **2014**, *751*, 174. (b) Kotani, H.; Sugiyama, T.; Ishizuka, T.; Shiota, Y.; Yoshizawa, K.; Kojima, T. *J. Am. Chem. Soc.* **2015**, *137*, 11222.

(11) (a) Schley, N. D.; Blakemore, J. D.; Subbaiyan, N. K.; Incarvito, C. D.; D'Souza, F.; Crabtree, R. H.; Brudvig, G. W. *J. Am. Chem. Soc.* **2011**, *133*, 10473. (b) Hintermair, U.; Hashmi, S. M.; Elimelech, M.; Crabtree, R. H. *J. Am. Chem. Soc.* **2012**, *134*, 9785. (c) Hintermair, U.; Sheehan, S. W.; Parent, A. R.; Ess, D. H.; Richens, D. T.; Vaccaro, P. H.; Brudvig, G. W.; Crabtree, R. H. *J. Am. Chem. Soc.* **2013**, *135*, 10837. (d) Thomsen, J. M.; Sheehan, S. W.; Hashmi, S. M.; Campos, J.; Hintermair, U.; Crabtree, R. H.; Brudvig, G. W. *J. Am. Chem. Soc.* **2014**, *136*, 13826. (e) Sheehan, S. W.; Thomsen, J. M.; Hintermair, U.; Crabtree, R. H.; Brudvig, G. W.; Schmuttenmaer, C. A. *Nat. Commun.* **2015**, *6*, 6469.

(12) Bano, K.; Zhang, J.; Bond, A. M.; Unwin, P. R.; Macpherson, J. V. *J. Phys. Chem. C* **2015**, *119*, 12464.

(13) Tamayo, A. B.; Alleyne, B. D.; Djurovich, P. I.; Lamansky, S.; Tsyba, I.; Ho, N. N.; Bau, R.; Thompson, M. E. *J. Am. Chem. Soc.* **2003**, *125*, 7377.

(14) Lever, A. B. P. *Inorg. Chem.* **1990**, *29*, 1271.

DOI: 10.1021/jacs.5b12148
J. Am. Chem. Soc. 2015, 137, 15692−15695